京都大学防災研究所年報　第47号B　平成16年4月
Annuals of Disas. Prev. Res. Inst., Kyoto Univ., No. 47 B, 2004

WAVELET-BASED MULTIFRACTAL ANALYSIS OF REAL AND SIMULATED TIME SERIES OF EARTHQUAKES

Bogdan ENESCU[*,**], Kiyoshi ITO, and Zbigniew R. STRUZIK[***]

[*]Research Center for Earthquake Prediction, Disaster Prevention Research Institute (DPRI), Kyoto University, Kyoto, Japan
[**]National Institute for Earth Physics, Bucharest, Romania
[***]Centre for Mathematics and Computer Science (CWI), Amsterdam, The Netherlands

Synopsis

This study introduces a new approach (based on the *Continuous Wavelet Transform Modulus Maxima* method) to describe qualitatively and quantitatively the complex temporal patterns of seismicity, their multifractal and clustering properties in particular. Firstly, we analyse the temporal characteristics of intermediate depth seismic activity in the Vrancea region, Romania. The second case studied is the shallow, crustal seismicity, which occurred in a relatively large region surrounding the epicentre of the 1995 Kobe earthquake. In both cases we have declustered the earthquake catalogue before analysis. The results obtained in the case of the Vrancea region show that for a relatively large range of scales, the process is nearly monofractal and random (does not display correlations). For the second case, two scaling regions can be readily noticed. At small scales the series display multifractal behaviour, while at larger scales we observe monofractal scaling. The Hölder exponent for the monofractal region is around 0.8, which would indicate the presence of long-range dependence (*LRD*). This result might be the consequence of the complex oscillatory or power law trends of the analysed time series. In order to clarify the interpretation of the above results, we consider two "artificial" earthquake sequences. Firstly, we generate a "low productivity" earthquake catalogue, by using the *ETAS* model. The results, as expected, show no significant *LRD* for this simulated process. We also generate an event sequence by considering a cellular fault embedded in a 3-D elastic half-space. The series display clear quasi-periodic behaviour, as revealed by simple statistical tests. The result of the wavelet-based multifractal analysis shows several distinct scaling domains. We speculate that each scaling range corresponds to a different periodic trend of the time series.

Keywords: Real and synthetic earthquake sequences, (Multi)Fractals, Wavelet analysis, Long-range dependence, Earthquake prediction

1. Introduction

The notion of scaling is defined loosely as the absence of characteristic scales of a time series. Its main consequence is that the whole and its parts cannot be statistically distinguished from each other. The absence of such scales requires new signal processing tools for analysis and modelling. The *exact self-similar*, scale-invariant processes, like for example the fractional Brownian motion, are mathematically well defined and well documented. In actual real world data, however, the scaling holds only within a finite range and will typically be approximate. Therefore, other "scaling models" are more appropriate to describe their complexity. *Long-range dependence* (*LRD*) or long memory is a model for scaling observed within the limit of the largest scales. Research on *LRD* (or *long-range correlation*) characteristics of "real" time series is the subject of active research in fields ranging from genetics to network traffic modelling. Another broad class of signals corresponds to "*fractal processes*", which are usually related to scaling in the limit of small scales. Such time series are described by a (local) scaling exponent, which is related to the degree of regularity

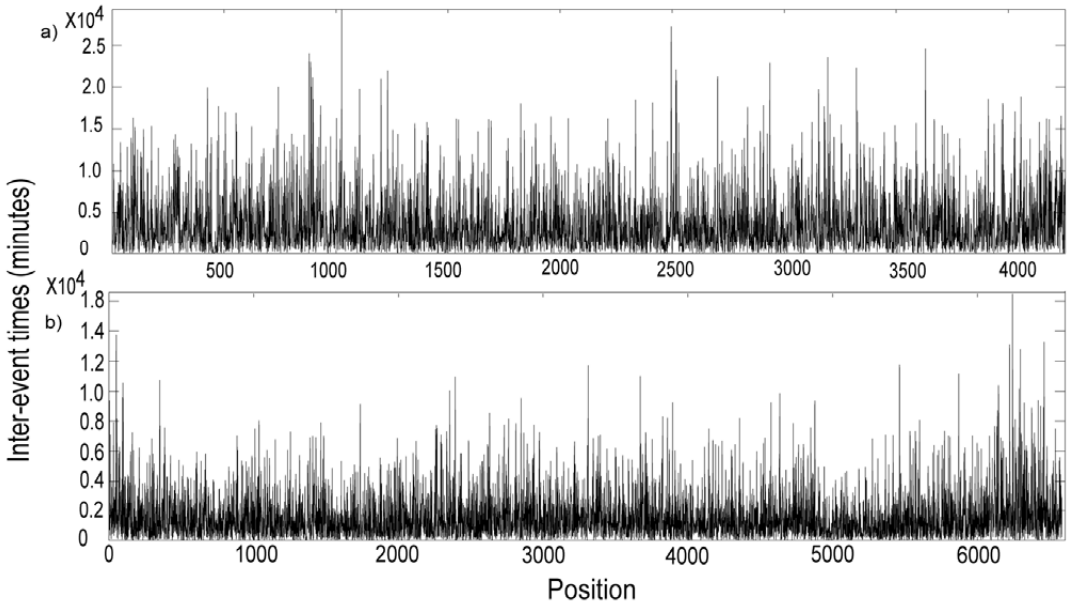

Fig. 1 Records of inter-event times, i.e. earthquake intervals, in the case of a) Vrancea (Romania) earthquakes; b) the shallow seismicity in the Hyogo region.

of a signal. If the scaling exponent varies with position (time), we refer to the corresponding process as multifractal. The fractal concept is, however, usually used in a broader sense and refers to any process that shows some sort of self-similarity.

(Multi)fractal structures have been found in various contexts, as for example in the study of turbulence or of stock market exchange rates. The concepts of "fractal analysis" have also been applied to describe the spatial and temporal distribution of earthquakes (e.g. Smalley et al., 1987; Turcotte, 1989 and Kagan and Jackson, 1991). Geilikman et al. (1990), Hirabayashi et al. (1992) and Goltz (1997) have all employed a multifractal approach to characterize the earthquake spatial, temporal or energy distribution. Their results suggest that seismicity is an inhomogeneous fractal process. Kagan and Jackson (1991), by analysing statistically several instrumental earthquake catalogues, concluded that besides the short-term clustering, characteristic for aftershock sequences, there is a long-term earthquake clustering in the residual (declustered) catalogues.

Wavelet analysis is a powerful technique, well suited to understanding deeply the complex features of real world processes: different "kinds" of

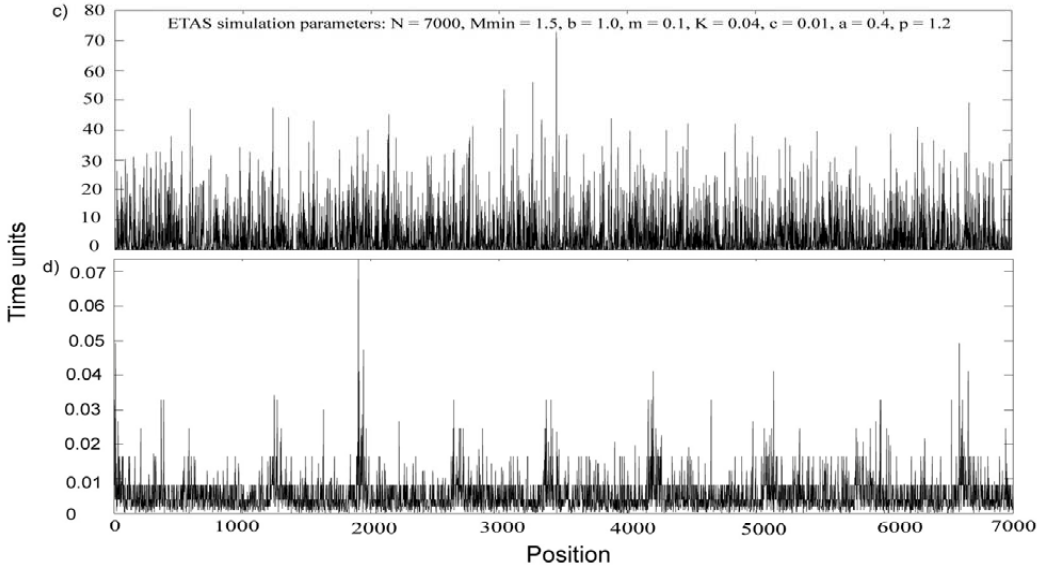

Fig. 1 Inter-event time series in the case of c) ETAS model simulation and d) EBZ_A simulation. For case d) only 7000 earthquake intervals were represented to show clearly the temporal pattern.

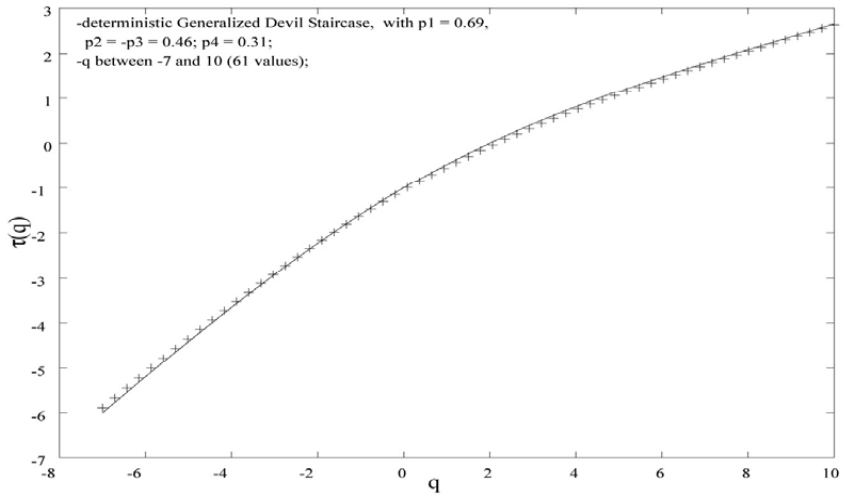

Fig. 2 "Tau spectrum" for the Generalised Devil Staircase. P1, p2, p3 and p4 are the parameters used to obtain the time series. *q* takes 61 equally spaced values, between -7 and 10. The scaling range fitted to compute this spectrum extends between 2^2 and 2^9. The theoretical spectrum (continuous line) and the computed one (small crosses) are in very good agreement.

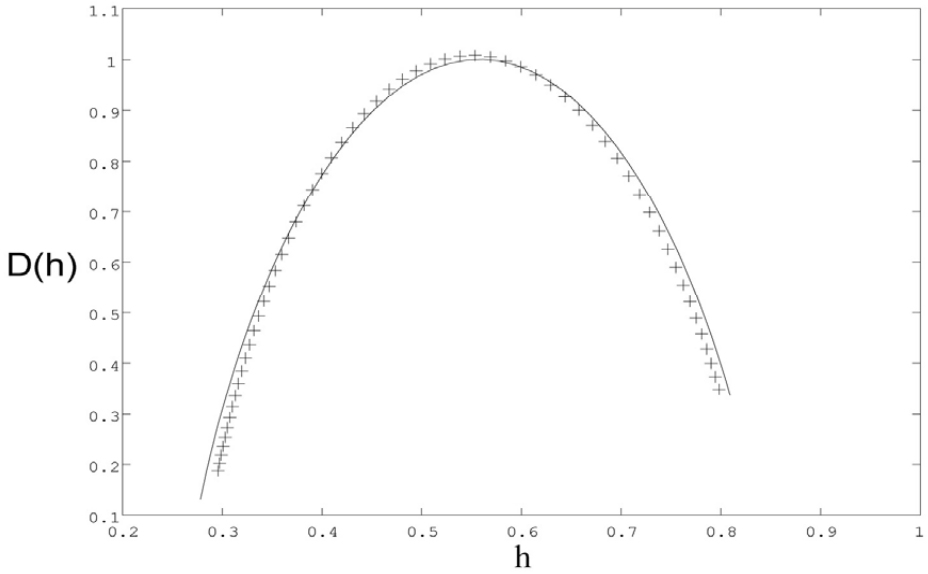

Fig. 3 Theoretical (continuous line) and obtained (crosses) *D(h)* multifractal spectrum in the case of the Multinomial Cantor Measure. One can notice the clear multifractal signature of the simulated time series, as well as the good agreement between the theoretical and computed spectrum.

(multi)fractality, *LRD*, non-stationarity, oscillatory behaviour and trends. The purpose of this study is to apply wavelet analysis to reveal the multifractal and *LRD* characteristics of the occurrence times of earthquakes. More precisely, we apply the wavelet transform modulus maxima (*WTMM*) method that has been proposed as a generalization of the multifractal formalism from singular measures to fractal distributions, including functions (Arneodo et al., 1991, Muzy et al., 1994 and Arneodo et al., 1995). By using wavelet analysis, we reveal the clear fractal characteristics of the analysed time series and successfully describe the main features of our earthquake sequences. The study focuses on the interpretation and explanation of the various temporal fractal patterns found in earthquake time series and thus, we hope, will be useful for future related studies. To the best of our knowledge, this is the first systematic study of the multifractal and *LRD* properties of earthquake time series by using a wavelet approach. Ouillon and Sornette (1996) have developed a wavelet-based approach to perform

multifractal analysis, and applied it in a related field: the study of earthquake fault patterns.

In the next chapter we introduce the *WTMM* method and explain the relation between multifractality and wavelets. The data to be analysed are introduced in chapter 3 and consist of four earthquake time series. Two of them are real earthquake sequences, while the other two are simulations. Firstly, we generate a sequence of events by using the *ETAS* model (Ogata, 1985, 1988). The second "artificial" time series is obtained by using a realistic earthquake model: an inhomogeneous cellular fault embedded in a three-dimensional elastic solid (Ben-Zion and Rice, 1993, Ben-Zion, 1996).

2. The Continuous Wavelet Transform (*CWT*) and wavelet-based multifractal analysis

The wavelet transform is a convolution product of the data sequence (a function f(x), where x, referred to in this study as "position", is usually a time or space variable) with the scaled and translated version of the mother wavelet, $\psi(x)$. The scaling and translation are performed by two parameters; the scale parameter s stretches (or compresses) the mother wavelet to the required resolution, while the translation parameter b shifts the analysing wavelet to the desired location:

$$(Wf)(s,b) = \frac{1}{s}\int_{-\infty}^{+\infty} f(x)\psi^*\left(\frac{x-b}{s}\right)dx, \qquad (1)$$

where s, b are real, $s > 0$ for the continuous version (CWT) and ψ^* is the complex conjugate of ψ. The wavelet transform acts as a microscope: it reveals more and more details while going towards smaller scales, i.e. towards smaller s values.

The mother wavelet ($\psi(x)$) is generally chosen to be well localised in space (or time) and frequency. Usually, $\psi(x)$ is only required to be of zero mean, but for the particular purpose of multifractal analysis $\psi(x)$ is also required to be orthogonal to some low order polynomials, up to the degree n:

$$\int_{\infty}^{-\infty} x^m \psi(x)dx = 0, \qquad \forall m, \quad 0 \le m < n \qquad (2)$$

Thus, while filtering out the trends, the wavelet transform can reveal the local characteristics of a signal, and more precisely its singularities. (The Hölder exponent can be understood as a global indicator of the local differentiability of a function.) By preserving both scale and location (time, space) information, the *CWT* is an excellent tool for mapping the changing properties of non-stationary signals. A class of commonly used real-valued analysing wavelets, which satisfies the above condition (2), is given by the successive derivatives of the *Gaussian* function:

$$\psi^{(N)}(x) = \frac{d^N}{dx^N} e^{-x^2/2}, \qquad (3)$$

for which $n = N$. In this study, the analysing wavelet is the second derivative of the *Gaussian*. The computation of the *CWT* was carried out in the frequency domain, by using the *Fast Fourier Transform*. The time series were padded with zeros up to the next power of two to reduce the edge distortions introduced by the Fourier transform, which assumes the data is infinite and cyclic (Torrence and Compo, 1998).

It can be shown that the wavelet transform can reveal the local characteristics of f at a point x_o. More precisely, we have the following power law relation:

$$W^{(n)} f(s, x_0) \sim |s|^{h(x_0)} \qquad (4)$$

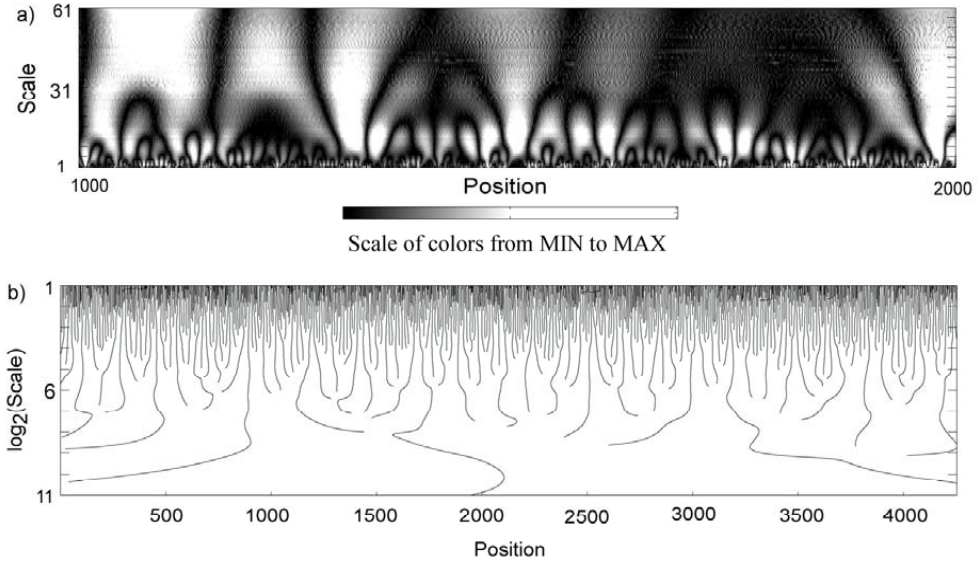

Fig. 4 a) CWT coefficients plot in the case of the Vrancea (Romania) time series, zoomed view. Scale and position are on the vertical and horizontal axis, respectively. The coefficients, taking values between *MIN* and *MAX*, are plotted by using 64 levels of grey. The plot was obtained by using the "Wavelet toolbox" of Matlab software. b) WTMM skeleton plot. The vertical axis is logarithmic, with small scales at the top.

where h is the Hölder exponent (or singularity strength). The symbol "*(n)*", which appears in the above formula, shows that the wavelet used ($\psi(x)$) is orthogonal to polynomials up to degree n (including n). The scaling parameter (the so-called *Hurst exponent*) estimated when analysing time series by using "monofractal" techniques is a global measure of self-similarity in a time series, while the singularity strength h can be considered a local version (i.e. it describes "local similarities") of the *Hurst exponent*. In the case of monofractal signals, which are characterised by the same singularity strength everywhere ($h(x) = ct$), the Hurst exponent equals h. Depending on the value of h, the input series could be long-range correlated (h > 0.5), uncorrelated (h = 0.5) or anti-correlated (h < 0.5).

The continuous wavelet transform described in Eq. (1) is an extremely redundant representation, too costly for most practical applications. To characterise the singular behaviour of functions, it is sufficient to consider the values and position of the Wavelet Transform Modulus Maxima (*WTMM*) (Mallat and Hwang, 1992). The wavelet modulus maxima is a point (s_0, x_0) on the scale-position plane, (s,x), where $|Wf(s_0, x)|$ is locally maximum for x in the neighbourhood of x_0. These maxima are located along curves in the plane (s,x). The *WTMM* representation has been used for defining the partition function-based multifractal formalism (Muzy et al., 1994, Arneodo et al., 1995).

Let $\{u_n(s)\}$, where n is an integer, be the position of all local maxima at a fixed scale s. By summing up the q's power of all these *WTMM*, we obtain the partition function Z:

$$Z(q,s) = \sum_n |Wf(u_n,s)|^q \qquad (5)$$

By varying q in Eq. (5), it is possible to characterise selectively the fluctuations of a time series: positive q's accentuate the "strong" inhomogeneities of the signal, while negative q's accentuate the "smoothest" ones. In this work, we have employed a slightly different formula to compute the partition function Z by using the "supremum method", which prevents divergences from appearing in the calculation of $Z(q,a)$, for $q < 0$ (e.g. Arneodo et al., 1995).

Often scaling behaviour is observed for $Z(q,s)$ and the spectrum $\tau(q)$, which describes how Z scales with s can be defined:

$$Z(q,s) \sim s^{\tau(q)} \qquad (6)$$

If the $\tau(q)$ exponents define a straight line, the analysed signal is a monofractal; otherwise the fractal properties of the signal are inhomogeneous, i.e. they change with location, and the time series is a multifractal. By using the Legendre transformation we can obtain the multifractal spectrum $D(h)$ from $\tau(q)$. $D(h)$ is a generalisation of the $f(\alpha)$ singularity spectrum (defined in the previous chapter) from measures to functions and captures how "frequently" a value h is found.

For the computations made in this work, we acknowledge the use of the *Matlab* software package (http://www.mathworks.com), Matlab's *Wavelet Toolbox* and the free software programs: *Wavelab* (Stanford University – http://www-stat.stanford.edu/~wavelab) (Buckheit and Donoho, 1995), *Fraclab, A Fractal Analysis Software* (INRIA - http://fractales.inria.fr/) and other *Matlab* routines (http://paos.colorado.edu/research/wavelets/; Torrence and Compo, 1998). We also developed

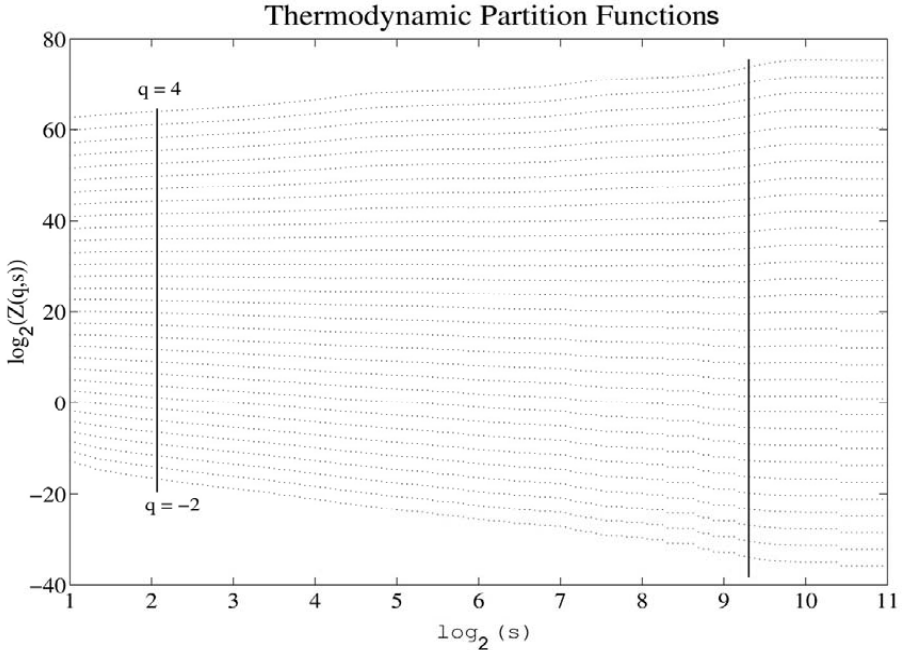

Fig. 5 Double-logarithmic plot of the partition functions, for q between 4 to -2 (up to down, constant increment), in the case of Vrancea time series. The vertical lines indicate the limits of the scaling region. Outside this area there are "edge effects" due to the limited length of the time series.

some routines, in *Matlab*, which are going to be made available on the web (http://www.rcep.dpri.kyoto-u.ac.jp/~benescu/).

3. Data

We have applied the wavelet-based approach to the analysis of four sets of earthquake data; two of them are real and the other two are simulations. The data consists of inter-event times between successive earthquakes above a threshold magnitude. Our choice was made by considering that the earthquake occurrence time is one of the most reliable and accurate parameters that define a seismic event. Also, our choice was based on the relevance of earthquake recurrence times for earthquake hazard and prediction. The results of the multifractal analysis ($\tau(q)$, $D(h)$) correspond, however, to the integrated inter-event times. In this way, we made our results directly comparable with those obtained by Enescu et al. (2003), who use the *Detrended Fluctuation Method* (*DFA*) to analyse the seismicity of the Vrancea (Romania) region. The method (*DFA*) requires integrating the data in advance. Nonetheless, the integration just adds a constant value (one) to the obtained h, the results being otherwise identical (Arneodo et al., 1995). The four sets of data are explained briefly below.

The Vrancea (Romania) region seismic activity

As a first application, we considered the intermediate depth seismicity (60-200 km depth) of the Vrancea region, Romania, between 1974-2002 (Fig. 1a). We have used an updated version of the Trifu and Radulian (1991) catalogue. The magnitude of completeness of the catalogue slightly increases with depth, being on average around 2.6 (Trifu and Radulian, 1991). Therefore, we have selected for analysis earthquakes with $M \geq 2.6$, and the resulting catalogue has 4,254 events. A detailed description of the catalogue and its main statistical features can be found in Trifu et al. (1990), Trifu and Radulian (1991) and Enescu et al. (2003).

The seismic activity before the 1995 Kobe earthquake

The second case studied is represented by the crustal seismic activity which occurred in the northern Hyogo area, Japan, from 1976 to January 17, 1995, the date of the Kobe earthquake (Mw = 6.9), in a broad area surrounding the epicentre of the big event (Fig. 1b). We have used the high quality earthquake catalogue of the Disaster Prevention Research Institute, Kyoto University, which for the area and period under investigation, is complete in earthquakes of magnitude $M \geq M_C = 1.5$. The data set (6,583 events) was thoroughly tested statistically by Enescu and Ito (2001) and, in his Ph.D. thesis, by Enescu (2004). Therefore we refer to these studies for further details.

ETAS model simulation

The *ETAS* (*Epidemic-Type Aftershock sequence*) model (Ogata, 1985, 1988) is a point process model representing the activity of earthquakes of magnitude *Mc* and larger occurring in a certain region during a certain interval of time. We have simulated such a process by using the following parameters: $Mc = 1.5$, $b = 1.0$, $\mu = 0.1$, $K = 0.04$. $c = 0.01$, $\alpha = 0.4$ and $p = 1.2$ (Fig. 1c). The first parameter represents the magnitude of completeness for the simulated data.

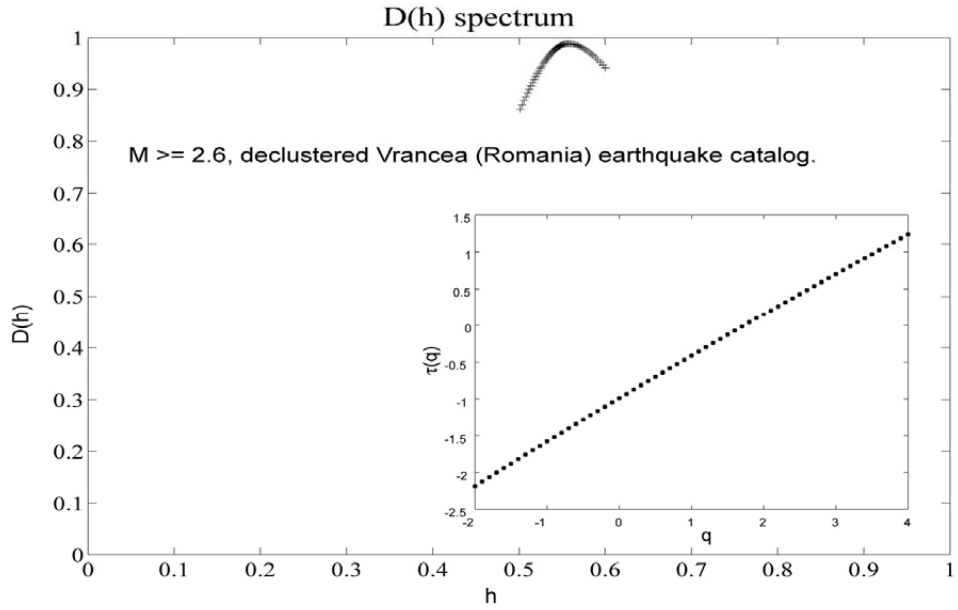

Fig. 6 *D(h)* spectrum of the integrated inter-event times, in the case of Vrancea (Romania) integrated earthquake intervals. The spectrum is quasi-monofractal, centered on 0.56. This value, slightly larger than 0.5, is an indication of quasi-randomness. The inset shows the $\tau(q)$ spectrum, which is very close to a straight line (an indication of monofractality).

The *b*-value is the slope of the frequency-magnitude distribution of earthquakes. The following five parameters represent the characteristics of earthquakes in the simulated time series. Among them, the last two parameters, α and *p*, are the most important in describing the temporal pattern of seismicity. Thus, the *p* value describes the decay rate of aftershock activity, and the α value measures the efficiency of an earthquake with a certain magnitude to generate offspring, or aftershocks, in a wide sense. For the physical interpretation of the other parameters and more details, we refer to Ogata (1992). In this study we have chosen a small α value to simulate a sequence of 7,000 events, with "low productivity" of aftershocks.

Simulation of seismicity by using a 2-D heterogeneous fault embedded in a 3-D elastic half space

The model we use (Ben-Zion, 1996) generates seismicity along a fault segment that is 70 km long and 17.5 km deep. The fault is divided into square cells with dimensions of 550 m. The boundary conditions and model parameters are compatible with the observations along the central San Andreas Fault. Eneva and Ben-Zion (1997) applied several pattern recognition techniques to examine four realisations of the model, with the same creep properties, but different brittle properties. The simulated catalogue of this study is identical to the case (A), described by Eneva and Ben-Zion (1997), and is the result of a fault model containing a Parkfield-type asperity of size 25 km X 5 km. From now on we will refer to this simulation as EBZ_A (25,880 events in total; Fig. 1d).

We decided to decluster both "real" earthquake catalogues before analysis (i.e. to eliminate the aftershock sequences from the catalogues) for two main reasons:

a) We are more interested in searching for *LRD* in the catalogue and therefore the elimination of shorter-range dependent seismicity (i.e. aftershocks) is considered appropriate, since it may influence the results on *LRD*.

b) The magnitude of completeness might be sub-evaluated immediately after the occurrence of some larger events, during the periods and in the regions under study. However, in the case of the intermediate-depth Vrancea earthquakes, the number of aftershocks is small even after major earthquakes, such as those that occurred in 1977 (Mw = 7.4), 1986 (Mw = 7.1) and 1990 (Mw = 6.9). For the crustal, shallow events in the Hyogo area, there are no major earthquakes during the period of investigation.

The declustering was done by using Reasenberg's (1985) algorithm in the case of the shallow events in the northern Kinki region (Enescu and Ito, 2001, Enescu, 2004). For the Vrancea (Romania) earthquakes a simplified declustering procedure was adopted, taking advantage of the scarcity of aftershocks for these intermediate-depth events (Enescu et al., 2003).

4 Results and discussion

Figure 1 shows the series of inter-event times between consecutive earthquakes for all four cases studied. The graphs look rather similar, with no clear distinctive characteristics. Only for the EBZ_A simulation (Fig. 1d), some kind of regular and quasi-periodic behaviour can be observed.

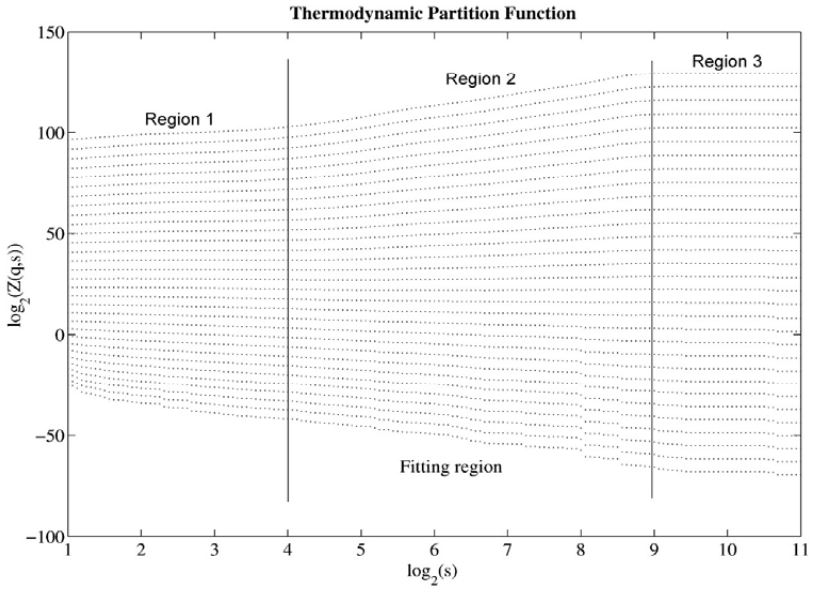

Fig. 7 Partition functions for *q* between 7 to -4 (from up to down, constant increment), for the case of the "Kobe time series". One can notice a clear crossover of scaling between Region 1 and Region 2. There is no reliable scaling in Region 3, due to the limited length of the data set.

Fig. 2 displays the "*tau spectrum, (τ(q)*", obtained by using the *WTMM* method, in the case of a "classic" example of a recursive fractal function: *the Generalized Devil's Staircase*, associated with the *Multinomial Cantor Measure*. The measure is constructed by dividing recursively the unit interval *[0, 1]* in four sub-intervals of the same lengths and distributing the "measure" or "mass" μ among them, with the weights *p1*, *p2*, *p3* and *p4* (*p1+p2+p3+p4 = 1*) (Peitgen et al., 1992, Appendix B). One can notice the very good agreement between the theoretical and the computed spectrum, for *q* values between –7 and 10. The spectrum is curved, which indicates the multifractal nature of the time series. By using the Legendre transform, we obtain the spectrum *D(h)*, represented in Fig. 3, which clearly confirms the non-uniqueness of the Hölder exponent *h*, and thus the multifractality of the process.

Figure 4a shows the *CWT* representation in the case of the Vrancea region earthquake intervals. A zoomed view is displayed in order to observe better the clear self-similar (*fractal*) pattern. From an intuitive point of view, the wavelet transform consists of calculating a "resemblance index" between the signal and the wavelet, in this case the second derivative of the *Gaussian*. If a signal is similar to itself at different scales, then the "resemblance index" or wavelet coefficients also will be similar at different scales. In the coefficients plot (Fig. 4a), which shows scale on the vertical axes, this self-similarity generates a characteristic pattern. We believe that this is a very good demonstration of how well the wavelet transform can reveal the fractal pattern of the seismic activity at different times and scales. Figure 4b displays the maxima lines of the *CWT* (i.e. the *WTMM* tree) in the case of the Vrancea time series. One can notice the branching structure of the *WTMM* skeleton, in the *(position, scale)* coordinates, which enlightens the hierarchical structure of time series singularities.

Figure 5 represents in a logarithmic plot the partition functions *Z (q,s)* versus scale *(s)*, obtained from the *WTMM* skeleton representation (Fig. 4b). One can notice the existence of a well-defined, relatively broad scaling region, as it is indicated in the figure. This scaling domain corresponds approximately to time periods from days to several years.

Figure 6 shows the *D(h)* plot in the case of the Vrancea (Romania) integrated inter-event times. The spectrum is narrow (i.e. the Hurst exponent (*h*) takes values in a very limited range). The τ spectrum, represented in the inset of the figure, can be well fitted by a straight line. These observations suggest that our time series is the result of a monofractal (or near-monofractal) process. One can also notice that the "central" *h* value of the spectrum is close to 0.5, which is an indication of the nearly random behaviour of the time series. Enescu et al. (2003) obtained a similar result, by using a "monofractal" approach, the *Detrended Fluctuation Analysis* (*DFA*) technique. We conclude that the defining temporal characteristics of the analysed data set (M ≥ 2.8) are mono-fractality and randomness. We cannot exclude, however, the existence of a non-random (quasi-periodic?) pattern for the major Vrancea earthquakes, as discussed by

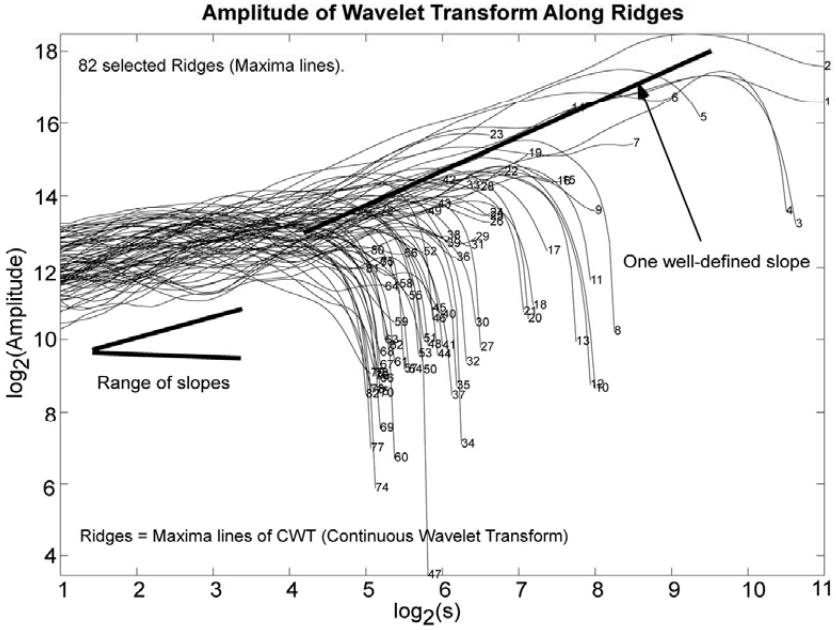

Fig. 8 Logarithmic plot of the Amplitude of CWT along ridges (maxima lines of the *Continuous Wavelet Transform*). At large scales there is only one well-defined, predominant slope of the lines, while at smaller scales there is a range of slopes. Because of the large number of WTMM lines, only a representative set was considered in this plot.

Enescu et al. (2003).

Figure 7 shows the partition functions *Z(q,s)* computed from the *WTMM* skeleton of the second time series considered here for analysis: the inter-event times of the "Kobe sequence". One can easily notice that there are two distinct, well-defined, scaling domains, at smaller scales and larger ones respectively, as indicated in the figure. Further evidence for the existence of these two scaling regions is presented in Fig. 8, which displays the amplitude of the *Wavelet Transform* along *Ridges* (i.e. maxima lines). As Eq. (4) also suggests, the slopes of these maxima lines correspond to the local Hölder exponents (or local singularities) of a time series. However, for most "real" signals, these "local" slopes are intrinsically unstable (mainly because the singularities are not isolated), thus making very difficult the estimation of these local exponents. In contrast, the partition function approach provides global estimates of scaling, which are statistically more robust. However, by closely examining Fig. 8, one can notice that again there is a rather clear crossover between small and large scales.

By computing the corresponding *D(h)* spectrum for each of the two scaling domains, at small scales ($2^1 \sim 2^4$) we observed multifractal behaviour, while at larger scales ($2^4 \sim 2^9$) the series is monofractal, with an exponent of about 0.8. The first scaling domain extends roughly from hours to days, while the second one corresponds to periods of time up to 2-3 years. As is known, $h > 0.5$ could indicate the presence of correlations (or long-range correlations), but there is also another important factor that can produce $h > 0.5$. It relates to the probability distribution of the time series (in our case the probability distribution of the inter-event times). Thus, for series with a power law like probability distribution (or other distributions characterised by heavy tails), one observes $h > 0.5$. A method to discriminate between *LRD* and the results of the probability distribution effects is to analyse the shuffled version of the signal. By shuffling the series, the correlation is lost but the power law like distribution, if present, remains unchanged. In other words, the shuffled series would have $h = 0.5$ in the first case (only *LRD*) and $h > 0.5$ in the second one (only power law like distribution). We shuffled our series and obtain $h = 0.5$, which excludes the possibility of an h larger than 0.5 caused by the probability distribution.

There is still one more factor that could "induce" *LRD*-like characteristics: the presence of trends within the data. As already mentioned, the wavelet approach eliminates the effect of polynomial trends, if an appropriate mother wavelet is used to compute the *CWT*. However, there are situations when other types of trends are present in the time series, like for example power law or oscillatory trends. As shown by Kantelhardt et al. (2001) and Hu et al. (2001), both kinds of non-stationarities, superposed on *LRD* data, could produce crossovers of the scaling region. By carefully analysing our sequence, we identified some oscillatory behaviour and also periods of "accelerating seismicity" or quiescence. As shown by Enescu and Ito (2001) and Enescu (2004) anomalous earthquake frequency

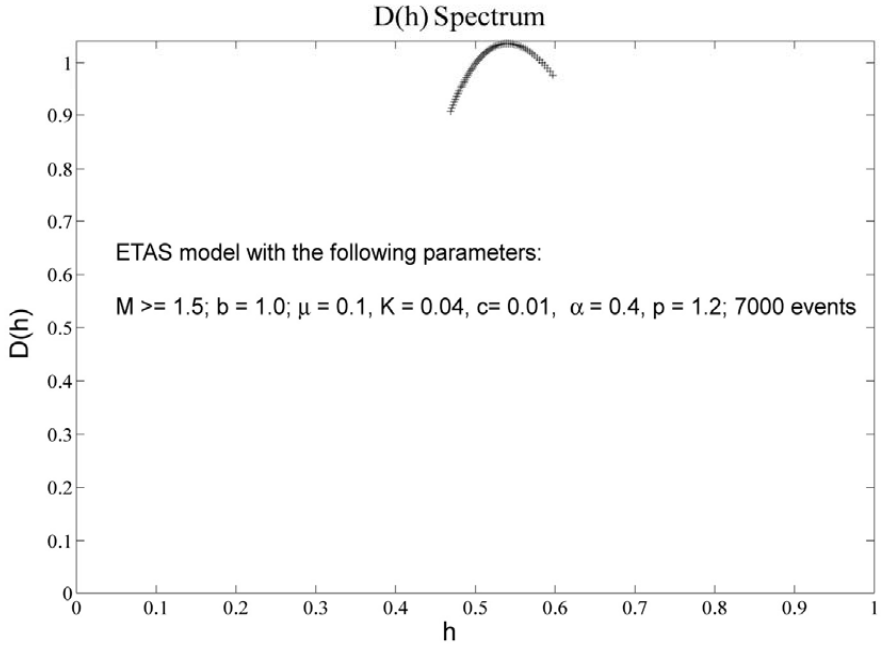

Fig. 9 Multifractal spectrum in the case of *ETAS* model simulation. By analysing the spectrum one can assume a quasi-monofractal, non-correlated process. A scaling range between 2^2 and 2^9 was used to compute the *D(h)* spectrum.

changes occurred several years before the 1995 Kobe earthquake. The increase and decrease of earthquake frequency could have been associated with power law (or higher order polynomial?) trends of the earthquake intervals. Therefore, it is possible that such rather complex non-stationary patterns are responsible for the large value of *h* and thus for the *LRD* signature obtained in this study. We would like to note, however, that while a clear distinction should be made between simple, trivial trends and genuine long-range dependence, such a separation is probably less definite in the case of trends having complex, low-frequency characteristics. On the other hand, more important to emphasise in our case is the existence of two distinct scaling domains, both of them associated with fluctuations that are *intrinsic* to the data. More research has to be done, however, to identify "the nature" of these fluctuations and their physical background.

The computation of the *D(h)* spectrum at small scales (2^1 to 2^4 ; see Fig. 7) showed multifractality, which probably corresponds to inhomogeneous local

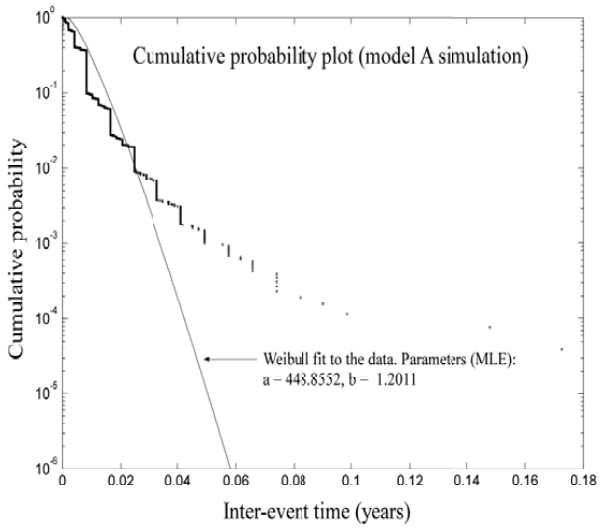

Fig. 10 Cumulative probability plot of inter-event times for EBZ_A simulation. A Weibull probability distribution is fitted to the data. The graph suggests the non-Poissonian character of the time series and the existence of quasi-periodicities (see text).

scaling behaviour of the time series. The result may also reflect the incomplete detection and removal of aftershocks. However, these findings are less reliable due to the limited length of the data set and a rather short scaling domain.

Our third case is concerned with the analysis of a simulated earthquake sequence, obtained by using the *ETAS* model. Figure 9 shows the *D(h)* spectrum computed by using a scaling region of the partition functions *Z* between 2^3 and 2^{10}. The plot shows a monofractal spectrum, with a Hurst exponent, *h*, close to 0.5. It is an expected finding for a sequence that has low offspring productivity and thus behaves quasi-randomly in the range of scales mentioned above. The result demonstrates that the small number of aftershocks, which occurred for very short periods of time, could not influence significantly the spectrum's characteristics at larger scales.

Our final analysis is concerned with another earthquake simulation, EBZ_A (see chapter 3). We are primarily interested here to see if oscillatory behaviour of the time series could induce a crossover of scaling and apparent long-range correlation. Figure 10 shows the result of basic statistical testing of data. We represent the cumulative probability distribution of the inter-event times in a half-logarithmic plot. A random occurrence of earthquakes corresponds to an exponential distribution of the inter-event times and, thus, in such a case, one would expect a straight line of the plot. The evident departure from linearity is a clear proof that the simulated earthquakes do not occur randomly. The step-like shape of the plot suggests that some recurrence intervals are strongly preferred, or in other words that our data has several quasi-periodicities.

Figure 11a presents the frequency of earthquakes versus time (the total time span of the earthquake sequence is 150 years). The graph confirms the periodic behaviour found before. We have also analysed the variation of CWT coefficients with time and found the same oscillatory behaviour. Fig. 11b displays the partition functions in the case of the EBZ_A simulation, only for *q = 2, 3 and 4*. As in the case of the "Kobe earthquake time series", one can see a segmented plot, which indicates different characteristics across scales. It is beyond the scope of this study to analyse in detail the influence of oscillatory trends on the multifractal characteristics of the analysed signal, as they are revealed by wavelet analysis. Some preliminary results, however, indicate that such a relation could be "quantified" and employed as a useful tool to analyse the behaviour of complex signals.

5. Conclusions

The present paper presents an in-depth analysis of the multifractal and correlation properties of real and simulated time series of earthquakes, using a wavelet-based approach. Our study reveals the clear fractal pattern of the analysed series of inter-event times and their different scaling characteristics.

In the case of the intermediate depth seismic activity in Vrancea, Romania, we found random and monofractal behaviour that occurs for a rather broad range of scales. The crustal seismic activity in the Hyogo area, Japan, has different characteristics, the most notable ones being the crossover in scaling and the long-range correlation signature observed at larger scales. It is not certain, however, what is the "nature" of this *LRD*-like behaviour. We believe that the complex non-stationarities of the data (trends) are responsible for this result. There is some evidence in support of our assumption, coming from theoretical studies of *LRD* with superposed oscillatory or power law trends.

The investigation of two simulated earthquake sequences helped to understand the fractal and correlation properties of the real data. Thus, the

analysis of the ETAS model sequence, with a "low productivity" of aftershocks, showed that the clustering which occurs "locally" does not have any influence on the results at larger scales. The investigation of the time series of earthquakes, simulated by using a cellular fault embedded in a 3-D elastic medium, revealed the quasi-cyclic behaviour of the earthquake occurrence. We have shown that there are several crossovers of scaling, which are probably associated with the oscillatory trends of the simulated sequence of earthquakes.

The fractal characteristics of our time series were mainly addressed in this study by computing "global estimates of scaling". However, by using a recently developed technique (Struzik, 1999), one can evaluate the Hölder exponent at an arbitrary location and scale. Such an approach has led to interesting findings in different fields, such as medicine (Ivanov et al., 1999) and the economy (Struzik, 2001). In our next studies we are planning to follow such a "local" approach to study the complexity of earthquake time series. Moreover, by using a 2-D wavelet transform, we would like to extend our research from time series to spatial patterns of seismicity.

Acknowledgements

We would like to thank Y. Ogata, Y. Ben-Zion and M. Anghel for useful discussions and for providing simulation software programs and data. We acknowledge the useful comments and suggestions of Y. Umeda, J. Mori, I. Kawasaki and I. Nakanishi. B.E. is grateful to the Japanese Ministry of Education for providing him a scholarship to study at Kyoto University, Japan.

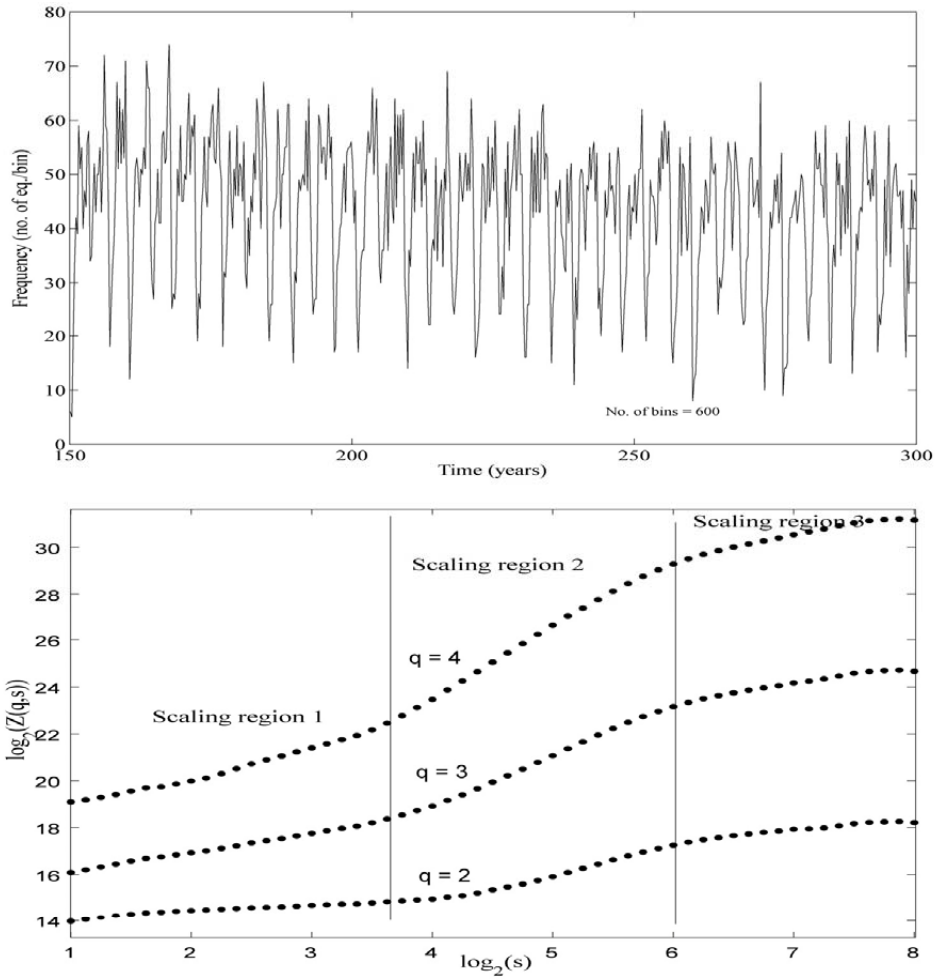

Fig. 11 a) Frequency of earthquakes versus time plot, in the case of *EBZ_A* simulation. Oscillatory behaviour is observed. b) Partition functions, Z, for q = 2, 3, 4, in the case of *EBZ_A* simulation. Several distinct scaling domains are observed. The vertical lines indicate the approximate borders of these regions.

References

Arneodo, A., Bacry, E., and Muzy, J.F. (1991): Wavelets and multifractal formalism for singular signals: application to turbulence data, *Phys. Rev. Lett.*, **67**, pp. 3515-3518.

Arneodo, A., Bacry, E. and Muzy, J.F. (1995): The Thermodynamics of Fractals Revisited with Wavelets, *Physica A*, 213, pp. 232-275.

Ben-Zion, Y. (1996): Stress, slip and earthquakes in models of complex single-fault systems incorporating brittle and creep deformations, *J. Geophys. Res.*, **101**, pp. 5677-5706.

Ben-Zion, Y. and Rice, J.R. (1993): Earthquake failure sequences along a cellular fault zone in a three-dimensional elastic solid containing asperity and non-asperity regions, *J. Geophys. Res.*, **98**, B8, pp. 14109-14131.

Buckheit, J.B., and Donoho, D.L. (1995): Wavelab and reproducible research, in A. Antoniadis and G. Oppenheim (Eds.), *Wavelets and Statistics* (pp. 55-81), New York, Springer Verlag.

Enescu, B. and Ito, K. (2001): Some premonitory phenomena of the 1995 Hyogo-ken Nanbu earthquake: seismicity, b-value and fractal dimension, *Tectonophysics*, **338**, 3-4, pp. 297-314.

Enescu, B., Ito, K., Radulian, M., Popescu, E. and Bazacliu, O. (2003): Multifractal and chaotic analysis of Vrancea (Romania) intermediate-depth earthquakes- Investigation of the temporal distribution of events-, *Pure and Appl. Geophys.* (in press).

Enescu, B. (2004): Temporal and spatial variation patterns of seismicity in relation to the crustal structure and earthquake physics, from the analyses of several earthquake sequences in Japan and Romania, Ph.D. thesis, Kyoto University, Kyoto, Japan.

Eneva, M., and Ben-Zion, Y. (1997): Application of pattern recognition techniques to earthquake catalogs generated by model of segmented fault systems in three-dimensional elastic solids, *J. Geophys. Res.*, **102**, B11, pp. 24513-24528.

Geilikman, M.B., Golubeva, T.V. and Pisarenko, V.F. (1990): Multifractal patterns of seismicity, *Earth and Planetary Science Letters*, **99**, pp. 127-132.

Goltz, C. (1997): Fractal and chaotic properties of earthquakes, Springer Verlag.

Hirabayashi, T., Ito K., and Yoshii, T. (1992): Multifractal analysis of earthquakes, *Pure and Appl. Geophys.*, **138,** 4, pp. 591-610.

Hu, K., Ivanov, P.Ch., Chen, Z., Carpena, P. and Stanley, H.E. (2001): Effect of trends on detrended fluctuation analysis, *Physical Review E*, **64**, 011114-1: 011114-19.

Ivanov, P. Ch., Amaral, L. A. N., Goldberger, A. L., Havlin, S., Rosenblum, M. G., Struzik, Z. R. and Stanley, H. E. (1999): Multifractality in human heartbeat dynamics, *Nature*, **399**, pp. 461-465.

Kagan, Y.Y., and Jackson, D.D. (1991): Long-term earthquake clustering, Geophys.J.Int., 104, pp. 117-133.

Kantelhardt, J.W., Koscienly-Bunde, E., Rego, H.H.A., Havlin, S. and Bunde, A. (2001): Detecting long-range correlations with detrended fluctuation analysis, *Physica A*, **295**, pp. 441-454.

Mallat, S. and Hwang, W.L. (1992): Singularity detection and processing with wavelets, *IEEE Trans. on Information Theory*, **38**, 2.

Muzy, J.F., Bacry, E., and Arneodo, A. (1994): The multifractal formalism revisited with wavelets, *Int. J. Bifurc. Chaos*, **4**, pp. 245-302.

Ogata, Y. (1985): Statistical models for earthquake occurrences and residual analysis for point processes, *Res. Memo.* (Technical Report) 288, Inst. Statist. Math., Tokyo.

Ogata, Y. (1988): Statistical models for earthquake occurrences and residual analysis for point processes, *J. Amer. Statist. Assoc.*, **83**, 9-27.

Ogata, Y. (1992): Detection of precursory relative quiescence before great earthquakes through a statistical model, *J. Geophys. Res.*, **97**, B13, pp. 19845-19871.

Ouillon, G. and Sornette, D. (1996): Unbiased multifractal analysis; application to fault patterns, *Geophys. Res. Lett.*, **23**, pp. 3409-3412.

Peitgen, H.O., Jurgens, H. and Saupe, D. (1992): Chaos and fractals. New frontiers of science, Springer Verlag, New York.

Torrence, C. and Compo, G.P. (1998): A practical guide to wavelet analysis, *Bulletin of the American Meteorological Society*, **79**, 1, pp. 61-78.

Reasenberg, P. (1985): Second-order moment of central California seismicity, 1969-1982, *J.Geophys. Res.*, **90**, B7, pp. 5479-5495.

Smalley, R.F., Jr, Chatelain, J.-L., Turcotte, D.L., and Prevot, R. (1987): A fractal approach to the clustering of earthquakes: applications to seismicity of the New Hebrides, *Bull. Seism. Soc. Am.*, **77**, pp. 1368-1381.

Struzik, Z.R. (1999): Local effective Hölder exponent: estimation on the Wavelet Transform Maxima tree. In Michel Dekking, Jacques Levy Vehel, Evelyne Lutton and Claude Tricot, *Fractals: Theory and Applications in Engineering*, pp. 93-112, Springer Verlag.

Struzik, Z.R. (2001): Wavelet methods in (financial) time series processing, *Physica A*, **296**, 1-2, pp. 307-319.

Trifu, C-I., and Radulian, M. (1991): Frequency-magnitude distribution of earthquakes in Vrancea: Relevance for a discrete model, *J. Geophys. Res.*, **96**, B3, pp. 4301-4311.

Trifu, C-I., Radulian, M., and Popescu, E. (1990): Characteristics of intermediate depth microseismicity in Vrancea region, *Rev. Geofis.*, **46**, pp. 75-82.

Turcotte, D.L. (1989): Fractals in geology and geophysics, Pure and Appl. Geophys., 131, pp. 171-196.

観測および人工地震系列に対するウェーブレット法に基づくマルチフラクタル解析

ボグダン，エネスク*、**・伊藤　潔・ズビグニェヴ，ストゥルズィク***

*　京都大学防災研究所地震予知研究センター
**　ルーマニア国立地球物理学研究所
***　数学および計算機センター（オランダ，アムステルダム）

要　旨

本論文では地震の時系列パターンの解析，特にマルチフラクタル解析にウェーブレット変換を導入した。最初にルーマニア，ブランチャ地方における中深発地震の解析を行い，次に1995年兵庫県南部地震付近のやゝ広範囲に発生する浅発地震の解析を行った。両解析にはデクラスターを施したデータセットを用いた。前者のルーマニアにおける地震はモノフルクタルでランダムであるという結論を得た。しかし，後者では大小２つのスケールにおいて，違ったフラクタル構造を示す。すなわち，小さなスケールではマルチフラクタル構造，大きいスケールではモノフラクタル構造を示すことがわかった。また，大きいスケールでのホルダーべき係数は0.8であり，これは長期記憶過程（LRD = long-range dependence）を　示すものである可能性がある。
これを調べるためにさらに２つの人工的な時系列を作り同じような解析を行った。一つはETASモデルに基づくもので，予想通り有意なLRDは見いだせなかった。もう一つは３次元半無限媒質中におけるcellular　faultによる時系列である。この時系列は明瞭な擬似周期性を示すことがわかった。これらのことから，マルチフラクタル構造が示す違ったスケールが異なった周期の活動パターンを示すことが推測される。

キーワード：地震系列，マルチフラクタル，ウェーブレット解析，長時間記憶過程，地震予知，地震統計